Global Change Biology
celebrating 20 years

Global Change Biology (2014), doi: 10.1111/gcb.12556

Divergent phenological response to hydroclimate variability in forested mountain watersheds

TAEHEE HWANG[1], LAWRENCE E. BAND[1,2], CHELCY F. MINIAT[3], CONGHE SONG[2], PAUL V. BOLSTAD[4], JAMES M. VOSE[5] and JASON P. LOVE[6]

[1]*Institute for the Environment, University of North Carolina at Chapel Hill, Chapel Hill, NC 27599, USA,* [2]*Department of Geography, University of North Carolina at Chapel Hill, Chapel Hill, NC 27599, USA,* [3]*Coweeta Hydrologic Laboratory, USDA Forest Service, Otto, NC 28763, USA,* [4]*Department of Forest Resources, University of Minnesota, Saint Paul, MN 55108, USA,* [5]*Center for Integrated Forest Science and Synthesis, USDA Forest Service, Raleigh, NC 27695, USA,* [6]*Warnell School of Forestry and Natural Resources, University of Georgia, Athens, GA 28763, USA*

Abstract

Mountain watersheds are primary sources of freshwater, carbon sequestration, and other ecosystem services. There is significant interest in the effects of climate change and variability on these processes over short to long time scales. Much of the impact of hydroclimate variability in forest ecosystems is manifested in vegetation dynamics in space and time. In steep terrain, leaf phenology responds to topoclimate in complex ways, and can produce specific and measurable shifts in landscape forest patterns. The onset of spring is usually delayed at a specific rate with increasing elevation (often called Hopkins' Law; Hopkins, 1918), reflecting the dominant controls of temperature on greenup timing. Contrary with greenup, leaf senescence shows inconsistent trends along elevation gradients. Here, we present mechanisms and an explanation for this variability and its significance for ecosystem patterns and services in response to climate. We use moderate-resolution imaging spectro-radiometer (MODIS) Normalized Difference Vegetation Index (NDVI) data to derive landscape-induced phenological patterns over topoclimate gradients in a humid temperate broadleaf forest in southern Appalachians. These phenological patterns are validated with different sets of field observations. Our data demonstrate that divergent behavior of leaf senescence with elevation is closely related to late growing season hydroclimate variability in temperature and water balance patterns. Specifically, a drier late growing season is associated with earlier leaf senescence at low elevation than at middle elevation. The effect of drought stress on vegetation senescence timing also leads to tighter coupling between growing season length and ecosystem water use estimated from observed precipitation and runoff generation. This study indicates increased late growing season drought may be leading to divergent ecosystem response between high and low elevation forests. Landscape-induced phenological patterns are easily observed over wide areas and may be used as a unique diagnostic for sources of ecosystem vulnerability and sensitivity to hydroclimate change.

Keywords: drought deciduousness, hydroclimate variability, landscape phenology, MODIS NDVI, topoclimate gradient

Received 8 July 2013; revised version received 30 January 2014 and accepted 12 February 2014

Introduction

Forest mountain watersheds are important sources of ecosystem services, including their important role in regulating surface water quantity and quality, and carbon sequestration (Schimel *et al.*, 2002; Viviroli *et al.*, 2007). The structure and function of ecosystems vary significantly with topoclimate, and their sensitivity to climate change is a key concern. Vegetation phenology has been cited as a key, observable element in ecosystem response to climate change (Menzel *et al.*, 2006), as well as a major determinant of coupled land surface carbon and water exchange (Barr *et al.*, 2004; Richardson *et al.*, 2010), and species distributions (Chuine & Beaubien, 2001). Changes in vegetation phenology, specifically earlier leaf greenup and delayed senescence have been related to increased carbon uptake in deciduous biomes (Goulden *et al.*, 1996; Churkina *et al.*, 2005). It is usually assumed that mid- and high-latitude forest phenology is primarily determined by temperature and photoperiod, while seasonal rainfall is a more important factor in tropical and semiarid regions (Jolly *et al.*, 2005).

Warmer temperature may lead to an extended growing season for temperate deciduous forests by earlier greenup and delayed senescence. Lengthened growing season length (GSL) may increase ecosystem water use offsetting the effect of elevated CO_2 on stomatal conductance, but it may be difficult to generalize

Correspondence: Taehee Hwang, tel. 919 843-5680, fax 919 962-0353, e-mail: h7666@email.unc.edu

(Hanninen & Tanino, 2011). For example, Zhang *et al.* (2007) showed that warmer temperature can delay greenup in lower latitudes (40°N southward), where the requirement for winter chilling has not been met under recent climate warming (Schwartz & Hanes, 2010). In addition, the earlier greenup could be offset by increased water stress toward the late growing season (White & Nemani, 2003; Hu *et al.*, 2010), in which case the GSL and evapotranspiration (ET) would be constrained by water availability. Therefore, identifying key environmental constraints on leaf phenology is important to understanding ecosystem responses to climate change.

Many field studies have documented earlier leaf development with increasing temperature in temperate and cold regions, while no consistent trend has been found in leaf senescence (Chen *et al.*, 1999; Black *et al.*, 2000; Estrella & Menzel, 2006; Menzel *et al.*, 2006). Analysis of long-term global satellite images (e.g. advanced very high-resolution radiometers) also revealed asymmetric temporal trends in leaf greenup and senescence during the global warming era. Jeong *et al.* (2011) recently showed that global trends at start and end of growing season are very heterogeneous in a continental scale over the period 1982–2008. Dragoni & Rahman (2012) recently reported wide-spread delays in the end of growing season in deciduous forests of the Eastern USA from 1989 to 2008, which delay rates were negatively correlated with latitudes. Researchers also have recognized that leaf senescence does not show consistent trends along altitudinal and latitudinal gradients in temperate forests (Estrella & Menzel, 2006), despite several counter examples (e.g., Doi & Takahashi, 2008).

Asymmetric patterns between greenup and senescence have been also reported over local topoclimate gradients. The onset of spring generally showed linear delays with elevation increase in eastern US: 2.7 days per 100 m in New Hampshire (Richardson *et al.*, 2006) and 3.4 days per 100 m in North Carolina (Hwang *et al.*, 2011). This is often referred to as Hopkins' Law which posits a 1 day delay with every 30 m increase in elevation (Hopkins, 1918), and clearly indicates the dominant controls of temperature on the onset of spring. In contrast, leaf senescence has been reported to show nonlinear trends along elevation gradients both at the species and landscape levels. Vitasse *et al.* (2010) observed that leaf senescence timing showed hyperbolic patterns along an elevation gradient for European beech and oak species in common garden experiments. Hwang *et al.* (2011) analyzed the 10-year averaged landscape phenology from MODIS Normalized Difference Vegetation Index (NDVI) in southern Appalachians, and reported that leaf senescence showed a significant second order relationship with elevation. Elmore *et al.* (2012) found a stronger non-linear trend in senescence than in greenup along an elevation gradient estimated from Landsat images over last 25 years. These senescence trends often lead to similar nonlinear patterns in GSL along elevation gradients. However, these unexpected advances in leaf senescence at low elevations are not clearly understood.

Leaf senescence is a highly regulated physiological process that promotes plant survival, growth, and reproduction (Lers, 2007). It is also related to nutrient retranslocation and reductions in water stress at the whole-plant level (Marchin *et al.*, 2010). Therefore, multiple factors act on leaf senescence simultaneously depending on the phase of vegetation development (Partanen *et al.*, 1998). Accelerated leaf senescence associated with drought stress has been studied specifically in crops and grasslands (Rivero *et al.*, 2007), for which chemical mechanisms are largely known (Munne-Bosch & Alegre, 2004). Although several studies have reported early leaf senescence driven by extreme drought for temperate drought-deciduous trees (Pataki & Oren, 2003; Ford *et al.*, 2011a; Hoffmann *et al.*, 2011; Warren *et al.*, 2011; Gunderson *et al.*, 2012), the role and extent of drought stress in leaf phenology (especially leaf senescence) is not clearly understood. Furthermore, leaf senescence (especially coloration) is more difficult to monitor than greenup as recognition of color change can be often quite subjective. Leaf senescence models usually incorporate only temperature and photoperiod as model inputs (Delpierre *et al.*, 2009). However, they do not show comparable accuracy with greenup models, and are not applicable to some species (Vitasse *et al.*, 2011; Yang *et al.*, 2012).

There have been a few attempts to identify drought control on vegetation phenology in intra- and inter-site studies. Some studies reported that warm early growing season temperature was associated with advanced leaf coloring for some tree species (Kramer, 1995). Estrella & Menzel (2006) found that the number of dry days in summer was correlated with earlier leaf coloring for some species (e.g., birch). They also reported that warm May and June advanced leaf coloring for several species (e.g., horse chestnut, birch), while warm August and September usually delayed it. These could be interpreted as secondary effects of drought stress under dominant temperature controls on leaf senescence in temperate broadleaf forests. Drought stress may provide an important secondary influence that would be intensified with climate change and increased hydroclimate variability (O'Gorman & Schneider, 2009; Seager *et al.*, 2009). Recent studies demonstrate that global declines in net primary production and ET during the last decade are largely attributed to soil water

limitation (Jung *et al.*, 2010; Zhao & Running, 2010). The importance of drought stress has been emphasized in understanding ecosystem response to climate change as increased summer drought could counteract early spring carbon assimilation (Angert *et al.*, 2005) and increase tree mortality (Adams *et al.*, 2009) as temperature increases. However, few leaf senescence models for temperate broadleaf species incorporate drought stress as model input triggering drought-induced leaf senescence (Richardson *et al.*, 2006; Delpierre *et al.*, 2009).

In our previous paper (Hwang *et al.*, 2011), we reported the dominant topography-induced controls on leaf greenup and senescence and their asymmetric responses along an elevation gradient from 10-year averaged MODIS NDVI data. In this article, we further investigate the impact of interannual hydroclimate variability on patterns of leaf senescence along an elevation gradient in humid forest mountains. We hypothesize that the influence of drought stress on leaf senescence is not uniform over the landscape, and is leading to a divergence in forest phenology between high and low elevation ecosystems. The objectives of this article are to (1) estimate the landscape-level greenup and senescence patterns along an elevation gradient from MODIS NDVI, validated with different sets of field measurements, (2) determine leaf senescence response along an elevation gradient to interannual hydroclimate variability, and (3) examine the implications of this finding to understanding ecosystem response and vulnerability to climate change in southern Appalachian forests.

Methods and materials

Study area

Our study site is a forested mountain watershed of the Coweeta Hydrologic Laboratory, North Carolina, United States (Fig. 1). The study site has very steep topography with elevation ranging from 660 to 1590 m, providing highly variable yet distinct hydroclimate (e.g., temperature, radiation, and precipitation) within a small area (ca. 20 km^2). The climate is classified as marine, humid temperate. At the main climate station located in the valley floor (CS01/RG06; Fig. 1), long-term mean annual temperature is 12.6 °C, and has been increasing at 0.5 °C per decade since 1980 (Ford *et al.*, 2011b). Monthly mean temperature ranges from 3.6 °C in January to 20.2 °C in July. Temperature lapse rates are ca. 7 °C km^{-1} and 3 °C km^{-1} for max and min daily temperatures respectively (Bolstad *et al.*, 1998). Annual precipitation increases with elevation from 1870 mm at 685 m elevation to 2500 mm at 1430 m, about a 5% increase for every 100 m elevation increase (Swift *et al.*, 1988). Precipitation is distributed relatively evenly throughout the year, characterized by small, low-intensity rainfall events with less-than 2% falling as snow. The study site experienced a record-high wet year in 2009 (2375 mm yr^{-1} at RG06) and a severe drought in 2000 (1235 mm yr^{-1}), followed by a moderate drought in 2001

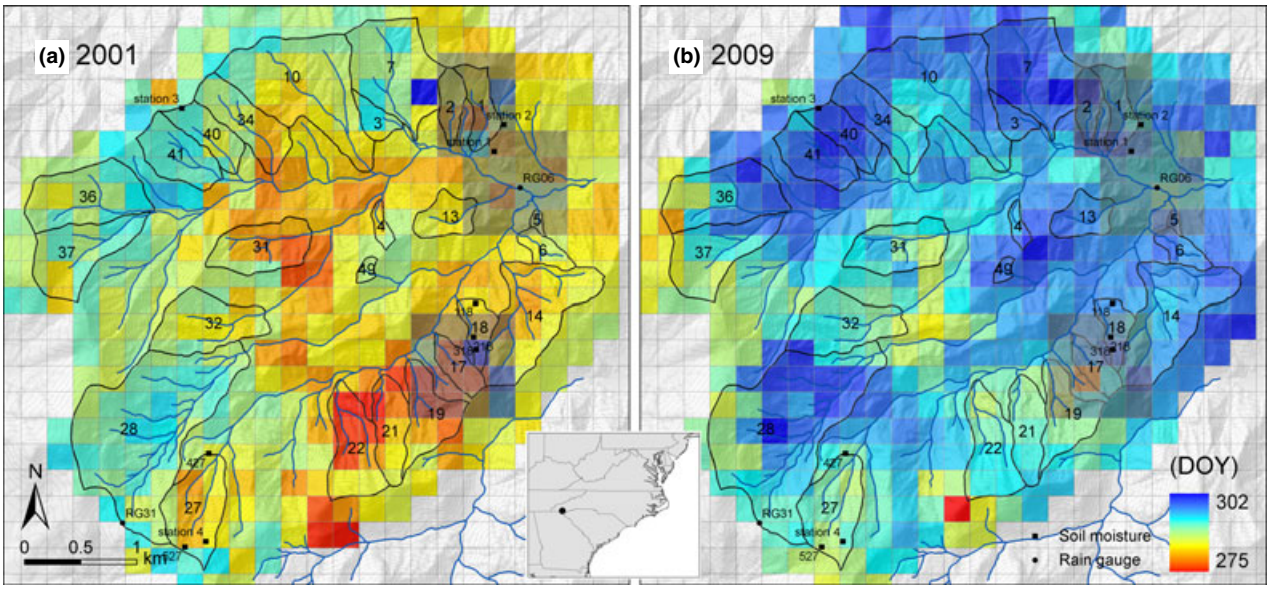

Fig. 1 Spatial patterns of the timing of MODIS-derived leaf senescence in (a) 2001 (a consecutive dry year) and (b) 2009 (a record-high wet year) within the study site (Coweeta Hydrologic Laboratory, NC, USA). Grids represent MODIS NDVI pixels (MOD13Q1; ca. 250 m). Black lines and numbers represent watershed boundaries and their ID numbers. Shaded grids are excluded in this study around lab facilities and watersheds 01/17, where white pine (*Pinus strobus L.*) was planted in 1957 and 1956 respectively. Contours are drawn at 20-m intervals.

(1395 mm yr^{-1}) (Fig. S1). Dominant canopy tree species are *Quercus* spp. (oaks), *Carya* spp. (hickory), *Nyssa sylvatica* (black gum), *Liriodendron tulipifera* (yellow poplar), and *Tsuga canadensis* (eastern hemlock). Northern hardwood forests occur at the highest elevation (ca. 1200 m above), including *Betula lutea* (black birch), *Tilia heterophylla* (basswood), *Aesculus octandra* (yellow buckeye), *Quercus rubra* (northern red oak), and *Acer saccharum* (sugar maple) (Day *et al*., 1988). Soils are relatively uniform, described as sandy loam inceptisols and ultisols typically of colluvial origin, with limited areas of deeper, more organic rich soils in coves (Hales *et al*., 2009). We use long-term hydrologic records of the low and high-elevation headwater catchments (WS18, mean elevation 823 m, and WS27, mean elevation 1256 m respectively) as representative of topoclimate and vegetation gradients in the study site (Fig. 1). These watersheds have been strictly preserved as control sites since the 1920s.

Landscape-scale phenology from MODIS NDVI

Recent developments in global satellite products (e.g. MODIS) provide medium-resolution vegetation dynamics to facilitate the study of landscape-scale vegetation phenology. These satellite-derived phenological products are well-correlated with ground-based observations of greenup and senescence in eastern US deciduous forests (Zhang *et al*., 2006; Liang *et al*., 2011; Zhang & Goldberg, 2011; Prebyl, 2012). We extracted spatial patterns of vegetation phenology using MODIS NDVI (MOD13Q1) from 2000 to 2011. Data were initially quality-controlled based on pixel reliability parameters, and post-processed (Hwang *et al*., 2011). A difference logistic function was used for extracting phenological signals from the time-series of MODIS NDVI (y) at day of year (DOY) t (Fisher *et al*., 2006) (Fig. S2):

$$y(t) = \left(\frac{1}{1+e^{a+bt}} - \frac{1}{1+e^{a'+b't}}\right)\cdot c + d \qquad (1)$$

where the fitted parameters a and b describe the greenup period (between greenup and maturity onsets), a' and b' for the senescence period (between senescence and dormancy onsets), d is the min NDVI value, and c is the difference between max and min NDVI. The coefficients are estimated in a nonlinear regression using iterative least squares estimation with *nlinfit* function in Matlab (The Mathworks Inc., Torrance, CA, United States). The mid-day of leaf greenup (Mid_{on}: DOY) and senescence (Mid_{off}: DOY) periods are calculated at each MODIS pixel to characterize phenological timing in this study, and are defined here as the inflection points of the model (White *et al*., 2009). GSL is defined as the number of days between Mid_{on} and Mid_{off} each year.

We analyzed leaf senescence patterns at three different elevation ranges (low: <800 m, middle: 900–1100 m, and high: >1200 m). The oak and mixed hardwoods dominate in mid- and low-elevation regions, while northern hardwood forests occur in the high-elevation (Day *et al*., 1988). We calculate the offset of leaf senescence at low (n = 41) compared with midelevation (n = 141) ('offset of leaf senescence at low elevation' hereon) to control for community composition (Mid_{off} at middle elevation − Mid_{off} at low elevation), and the confidence intervals of mean differences between the two groups with a paired t-test. The offset of leaf senescence at low elevation each year was then related to interannual hydroclimate variability during the late growing season (July–October) observed at low elevation (RG06). We also calculated Pearson correlation coefficients between anomalies of GSL and phenological variables (Mid_{on} and Mid_{off}) in all MODIS phenology data (3350 site-years), following Richardson *et al*. (2010). Anomalies were calculated each year (10 years) from mean values at each MODIS pixel (335 MODIS pixels). This analysis helps us to explore the determinants of GSL between greenup and senescence.

Spring and autumn phenology observations

Spring and autumn phenology have been measured weekly since 2003 at two walk-up towers on a low elevation (817 m) south-facing slope (station 2), and a high-elevation (1381 m) north-facing slope (station 4), ca. 200 m below a ridge (Fig. 1). Ten branches with different heights and species were marked at each tower (Table 1). Buds and leaves on the marked branches were categorized from stage 1 (winter stage) to 5 (fully elongated leaf) during the spring (typically starting in March and continuing until all leaves were fully elongated). During the fall, the percentage color change of leaves as well as percentage of leaf loss relative to the original branch coverage were assessed; measurements began in September, continuing weekly until complete leaf loss. All measurements were rescaled from 0 to 1 to form a phenological index, and analyzed together at each station to extract site-averaged phenological signals (Fig. S3).

The fraction of absorbed photosynthetically active radiation (FPAR) has been measured continuously at these sites since 2002 (Fig. S4). FPAR is a good indicator of absorbed energy by vegetation and subsequent carbon uptake; it is also linearly related to NDVI. Quantum sensors (LI-190SZ; LI-COR Inc., Lincoln, NE, USA) were installed both below and above the canopy. PAR was measured every minute, and hourly PAR sums were logged (CR10X; Campbell Scientific Inc., Logan, UT, USA). Hourly FPAR values are calculated from the ratio of below- to above-canopy PAR values. As hourly FPAR values fluctuate diurnally following solar geometry due to surrounding canopy and topographic shading, daily FPAR values were calculated only under low light conditions (20–120 μmol m^{-2} s^{-1}) to minimize shading effect, when diffuse radiation is dominant. We also apply the same logistic model into a single greenup or senescence phase of field observations at each station (Figs S3 and S4). It helps us to validate the MODIS-derived phenology at the same phase in the phenological trajectories.

Hydroclimate variables

Daily average temperature data from 12 locations within the study site (Table 2; Fig. 1) were used to calculate the cold degree-days at three elevation regions during the late

Table 1 Details for spring and autumn phenology measurements at two walk-up towers in the study site

Station	Branch Number	Height (m)	Species
2	1	4	*Nyssa sylvatica*
	2	5	*Nyssa sylvatica*
	3	6	*Acer rubrum*
	4	8	*Acer rubrum*
	5	8	*Oxydendrum arboreum*
	6	9	*Acer rubrum*
	7	9	*Quercus prinus*
	8	14	*Quercus prinus*
	9	15	*Quercus prinus*
	10	16	*Quercus prinus*
4	1	2	*Rhododendron calendulaceum*
	2	3	*Rhododendron calendulaceum*
	3	8	*Hamamelis virginiana*
	4	8	*Quercus prinus*
	5	10	*Amelanchier arborea*
	6	13	*Amelanchier arborea*
	7	15	*Quercus rubra*
	8	15	*Quercus prinus*
	9	15	*Quercus rubra*
	10	17	*Quercus prinus*

growing season (DOY 210–290). The cold degree-day (CDD_{Tb}) was defined as a thermal sum of the difference between daily average (T_{avg}) and threshold temperature (T_b; 20 °C in this study) between DOY_1 and DOY_2 according to (Richardson *et al*., 2006):

$$CDD_{T_b} = \sum_{DOY_1}^{DOY_2} \begin{bmatrix} (T_{avg} - T_b) & when & T_{avg} < T_b \\ 0 & when & T_{avg} \geq T_b \end{bmatrix} \quad (2)$$

Using daily base station precipitation and pan evaporation measurements (CS01/RG06; Fig. 1), we calculated total precipitation and seasonal water balance (total precipitation − pan evaporation) during the late growing season (July–October) to quantify interannual hydroclimate variability. We also used observed daily volumetric soil water content to assess the interannual hydroclimate variability (Fig. S6). These data have been collected in nine locations in the study site at different depths (0–30 and 30–60 cm), ranging from ridge to valley bottom (Table 2). The 60-cm measurement depths are close to observed rooting depths in the study site (Hwang *et al*., 2009). Plant water stress (ξ) was calculated over the 60 days before leaf senescence following (Rodriguez-Iturbe *et al*., 1999):

$$\xi = \begin{cases} \left[\frac{S^* - S}{S^* - S_{pwp}}\right]^q & when\ S < S^* \\ 0 & otherwise \end{cases} \quad (3)$$

where s is observed daily soil water content (V/V), s^* is the soil water content below which plants experience water stress, and s_{pwp} is the soil water content associated with the permanent wilting point of plants. The s^* and s_{pwp} parameters are defined as soil water content at the −3 and −0.03 MPa soil water pressure from the soil–moisture retention curves (Laio *et al*., 2001). The q parameter accounts for the nonlinear effect of soil water deficit on stomatal conductance, set to 2 in this study (Porporato *et al*., 2001).

Long-term vegetation phenology from GIMMS NDVI

We use the bimonthly 8-km Global Inventory Modeling and Mapping Studies (GIMMS) NDVI dataset to extract long-term phenological records (1982–2006) for the study site (Tucker *et al*., 2005). The whole study site is included in one 8-km GIMMS NDVI pixel. The same filtering and fitting techniques were applied to multiyear NDVI datasets to get max and min NDVI values (Hwang *et al*., 2011). The midpoint NDVI value was calculated from the average value between the max and min fitted NDVI values (White *et al*., 1997). The long-term

Table 2 Detailed information on weather stations, terrestrial gradient plots, and field stations

Site ID	Elevation (m)	Watershed ID	Hillslope position	Explanations
CS01/RG06	685	Base station	Bottom	Climate stations (CS)
CS05	1140	WS41	Ridge	Rain gauges (RG)
CS77	1430	WS27	Ridge	
RG31	1363	WS27	Ridge	
118	782	WS18	Ridge	Terrestrial gradient plots
218	795	WS18	Bottom	(temperature and soil moisture*)
318	865	WS18	Sideslope	
427	1001	WS27	Bottom	
527	1347	WS27	Ridge	
Station 1	739	Next to WS01	Bottom	Walk-up towers at stations
Station 2	821	Next to WS01	Ridge	2 and 4 for FPAR and phenology
Station 3	1226	WS40	Ridge	observations (temperature
Station 4	1383	WS27	Ridge	and soil moisture*)

*Soil moisture is measured at 0–60 cm depths (Fig. S6). Geographical locations of field sites are available in Fig. 1.

phenological records were extracted from the intersections between time-series NDVI lines and the midpoint NDVI value (Fig. S7), which showed a better agreement with MODIS-derived vegetation phenology than inflection points. This method was shown to be more closely related to ground observations compared to other satellite estimates for vegetation phenology (White *et al.*, 2009).

Although GIMMS NDVI provides long-term phenological patterns, they only provide an averaged ones in the study site. Therefore, we developed elevation-based phenology models for greenup and senescence to downscale the GIMMS NDVI derived vegetation phenology (8 km) to the medium-scale signals (250 m) using elevation and late growing season precipitation (July–October). MODIS-derived greenup and senescence timing was related to elevation at the 250-m scale each year. The first- ($y = ax + b$) and second-order ($y = ax^2 + bx + c$) polynomial equations with elevation were used for greenup and senescence, respectively, which showed better performance for multiyear NDVI datasets (Hwang *et al.*, 2011). The highest order (a) parameters were assumed constant in the downscaling process (verified later in this paper). The capability of detecting topography-induced vegetation phenology allowed us to convert long-term coarse-scale vegetation phenology to watershed-scale phenological signals.

Growing season evapotranspiration

Growing season ET was estimated each year from the mass balance of monthly precipitation and streamflow records (precipitation − streamflow). The water balance for gauged catchments can be simply written as:

$$P - Q = ET + \Delta S \quad (4)$$

where P is precipitation, Q is runoff, ET is evapotranspiration, and ΔS is the change in water storage. If ΔS is not accounted for, the mass-balance based ET underestimates ET during the growing season (Troch *et al.*, 2009), requiring a correction. During the dormant season in the study site (assuming low or negligible ET), precipitation is distributed between streamflow and recharge of the subsurface water deficit ($P = Q + \Delta S$), largely accumulated during the growing season. Therefore, the growing-season underestimate of ET by mass balance is approximately corrected by adding estimated monthly water balance ($P - Q$) beyond the end of the growing season, which is largely recharge (ΔS). Considering that the precipitation is evenly distributed throughout the year and there is rarely permanent snow pack in the study site, this provides a very efficient way to estimate the growing season ET. This catchment-scale water balance method was also previously validated with plot-scale sap flux measurements in the study site (Ford *et al.*, 2007).

Assuming monthly streamflow (Q) is a strong function of the level of storage (S) in the watersheds, we extend the periods of mass balance calculation for growing season ET until monthly streamflow was fully restored to the level of April, right before the growing season. In this way, we minimize transient effects of storage depletion during the growing season or even carry-over during the dormant season in growing season ET calculation [ΔS in Eqn (4)]. Boxplots of monthly precipitation and streamflow for low- (WS18) and high-elevation (WS27) catchments (Fig. 2) show that monthly streamflow usually reaches the same level as April by December in WS27, but not until January for WS18. Streamflow was fully restored in WS27 earlier than in WS18 due to higher precipitation, lower temperature, and a shorter growing season. Therefore, growing season ET was calculated from the period of May to December for WS27, and May to January for WS18. Major snow pack was not reported even at high elevation. The 1996–1998 years are excluded in this analysis as the study site experienced an unprecedented major wind storm (Hurricane Opal) on 5 October 1995, which resulted in significant canopy damage with a typical lag of a few years to close canopy gaps (Clinton & Baker, 2000; Elliott *et al.*, 2002).

Results

Validation of MODIS-derived vegetation phenology

MODIS-derived vegetation phenology showed relatively good agreement with ground-based estimates at the two walk-up towers. FPAR-derived Mid_{on} values showed the best agreement ($R^2 = 0.848$; *Mean Absolute Error* = 4.0 days; Fig. 3a), while the observed greenup timing was always earlier at both stations ($R^2 = 0.795$; $MAE = 9.1$ days; Fig. 3b). We observed a fairly consistent difference in greenup timing (Mid_{on}) between the two sites in most years (ca. 20 days), but not for senescence. Both FPAR- and abscission-based senescence (Mid_{off}) are usually 7–13 days later than those derived by leaf color and MODIS (Fig. 3d, f, g, and i). Mid_{off} values from the plot-scale FPAR and abscission observations showed the best agreement ($R^2 = 0.901$; $MAE = 2.8$ days; Fig. 3h). The highest correlation (R^2) and lowest mean absolute error values were found between MODIS and coloration-derived senescence ($R^2 = 0.732$; $MAE = 4.0$ days; Fig. 3e).

Greenup and senescence along the elevation gradient

From MODIS NDVI, we estimate spatial and temporal variations of landscape-level greenup, senescence, and subsequent GSL in the study site since 2000 (Fig. 4). MODIS-derived phenological dates (Mid_{on} and Mid_{off}) are well correlated with long-term vegetation phenology from GIMMS NDVI although there are consistent offsets in them. This may be attributed to differences in corresponding bandwidths between sensors (Gupta *et al.*, 2000; Teillet *et al.*, 2007). Leaf senescence showed more interannual variation than greenup both in MODIS Fig. 4) and GIMMS NDVI values (Fig. S7). Correlation coefficients for GSL anomalies with those of greenup and senescence were −0.39 and 0.75, respectively, indicating that senescence patterns in space and

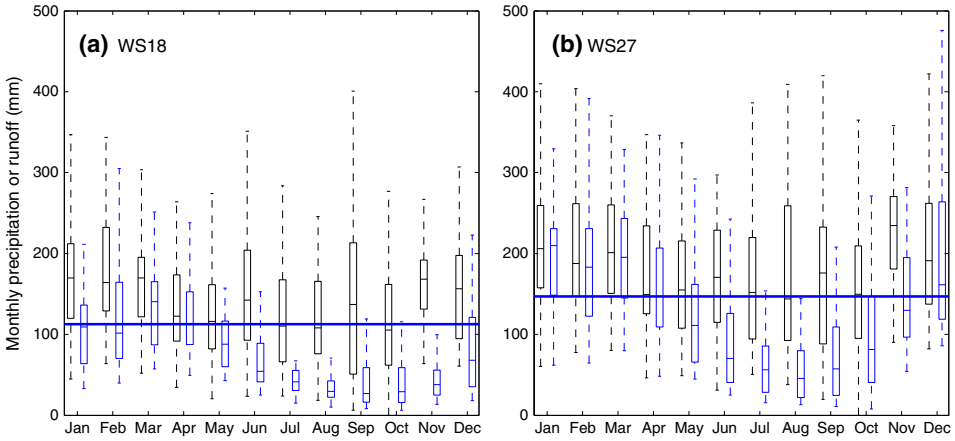

Fig. 2 Boxplots of monthly precipitation (black) and run-off generation (blue) for (a) low- (WS18, mean elevation: 823 m) and (b) high-elevation (WS27, mean elevation: 1256 m) catchments since 1982. Horizontal lines indicate the medium levels of observed streamflow in April, used to decide the timing of storage restoration after growing season.

time had a greater effect on canopy duration than greenup patterns in the study site.

The first and second-order phenology models with elevation for leaf greenup and senescence are shown in Fig. 5, all of which are statistically significant ($P < 0.005$). Second-order polynomial fits showed that leaf senescence generally exhibited distinct non-linear trends while linear trends were found in greenup (Fig. 5a and b). These quadratic senescence fits shifted both vertically and horizontally each year, while the linear greenup trends were relatively consistent. Note that there were distinct spatial patterns between dry (2001) and wet years (2009) at low elevation with early senescence in 2001 and delayed senescence in 2009 (Fig. 1). The highest-order parameters in greenup and senescence models did not show significant difference between years in their 95% confidence intervals, which supports the assumption in the downscaling process.

Hydroclimate controls on leaf senescence

In all elevation regions, leaf senescence timing showed significant linear relationships ($P < 0.001$) with cold degree-days at 20 °C (CDD_{20}) during the late growing season (Fig. 5c); however, the explanatory power of linear models (R^2) decreased with decreasing elevation. Senescence timing in the low-elevation region was earlier than the mid-elevation in most years although *CDD* values were consistently higher in the low-elevation. The sensitivity of senescence timing to CDD_{20} (featured by slopes of regression lines) was significantly different in the high elevation, where the northern hardwood occurs. We found significant negative linear relationships of the offset of leaf senescence at low elevation with late growing season precipitation and seasonal water balance (Fig. 6a and b). This indicates that a drier late growing season is associated with earlier leaf senescence at low elevation than at middle elevation. The offsets of leaf senescence at low elevation also show a significant nonlinear relationship with the 60-day sum of plant water stress before senescence (Fig. 6c). Note that the relationship with late growing season precipitation was also used to solve for the two parameters in second-order equation with elevation for senescence during the downscaling process.

The relationship between GSL and growing season ET

In most years, ET estimates were higher in the low-elevation catchment (WS18) than in the high-elevation catchment (WS27) by ca. 100 mm (Fig. 7). Growing season ET values generally increased with longer GSL in WS18 at ca. 4.3 mm per day ($R^2 = 0.440$, $P < 0.01$; Fig. 7a), while they showed a significant asymptotic pattern in WS27 ($R^2 = 0.508$, $P < 0.01$; Fig. 7b). The GSL-ET relationship shows a more scattered pattern and less significance in the drier catchment (WS18), where ET estimates might be more affected by errors in compensating for monthly storage depletion by ET [featured by ΔS in Eqn (4)]. In WS27, growing season ET remains steady between 600 and 700 mm even in years with long growing seasons (e.g. 1986). Considering that pan evaporation measurements at the base station (CS01; Fig. 1) show little interannual variation (Fig. S1), this asymptotic pattern indicates that the catchment might be more energy-limited than water-limited in those years. Interestingly, the GSL-ET measures in WS27 are far below the regression line in years after a hurricane Opal (1996–1998) and historic severe drought (2001) (Fig. 7b).

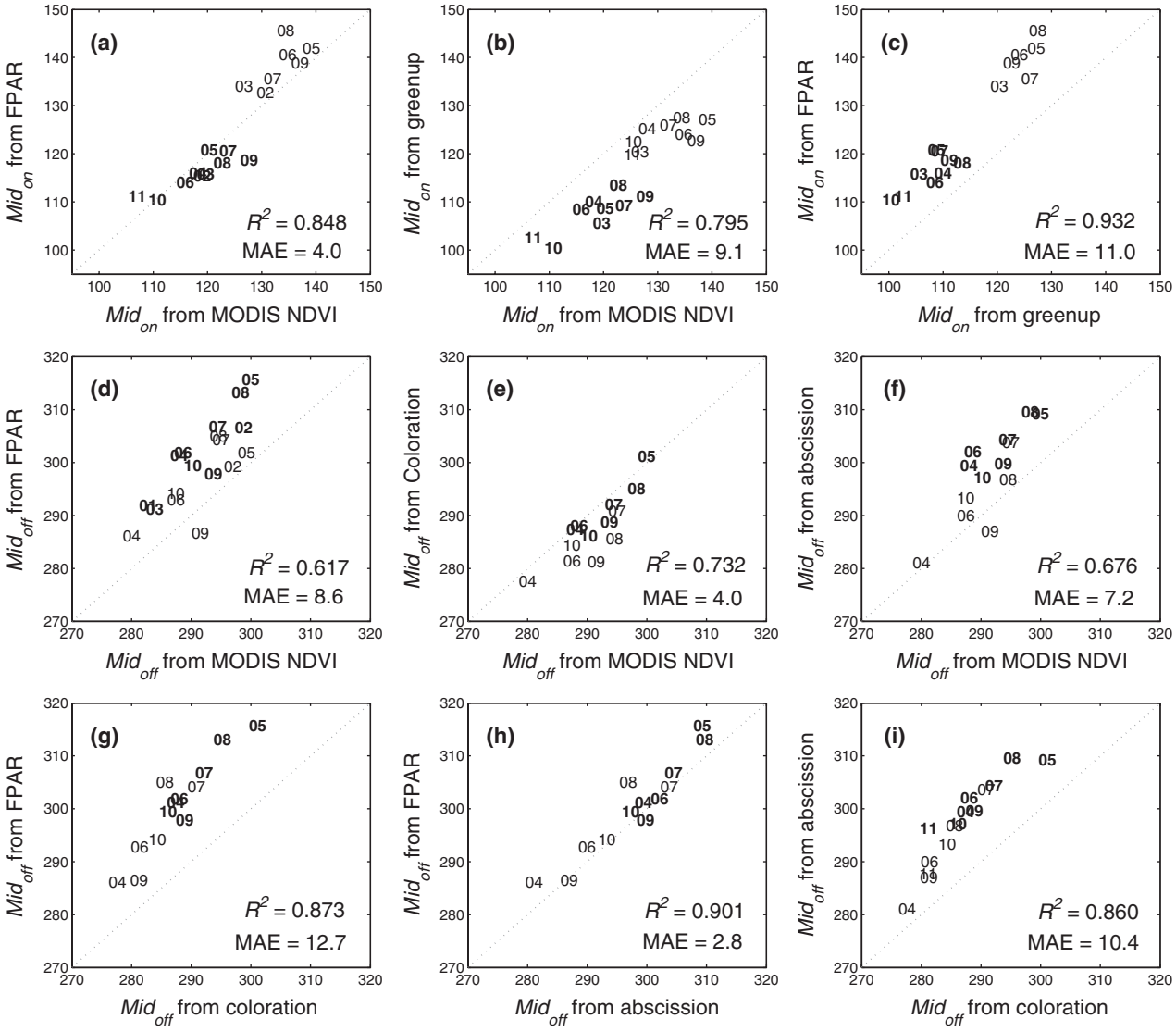

Fig. 3 The intercomparisons of mid-days of leaf greenup (Mid_{on}; day of year) and senescence (Mid_{off}; day of year), derived from time-series of MODIS NDVI (Fig. S2) and field observations (FPAR, greenup, coloration, and abscission; Figs S3 and S4) at two low- and high-elevation walk-up towers (stations 2 and 4; Table 2). Numbers represent the years from 2000. The numbers with bold character are for the station 2 (elevation 821 m), while those with normal character for the station 4 (elevation 1383 m; Fig. 1). MAE: mean absolute error (days).

Discussion and conclusions

MODIS-derived vegetation phenology

MODIS-derived Mid_{on} values showed a better agreement with field measurement of FPAR than weekly field observations of leaf elongation. This was probably due to either early assessments of fully elongated leaves or not considering leaf thickness change in field observations. However, MODIS-derived Mid_{off} values agreed better with coloration estimates than field measured canopy FPAR or abscission, potentially because colored leaves in branches still absorb or reflect significant portions of incoming PAR (Zhang & Goldberg, 2011; Gunderson *et al.*, 2012). Recently, Prebyl (2012) found that Mid_{on} values from eight MODIS pixels ranging in elevation from 690 to 1550 m in the study site had a MAE of 2.5 days with respect to field-based estimates from digital photographs, taken every 2 days from March through June at 30 sub-sampling points within each MODIS pixel.

We note that MODIS-derived senescence might show reduced sensitivity to hydroclimate variability and plant water stress compared with field measurements

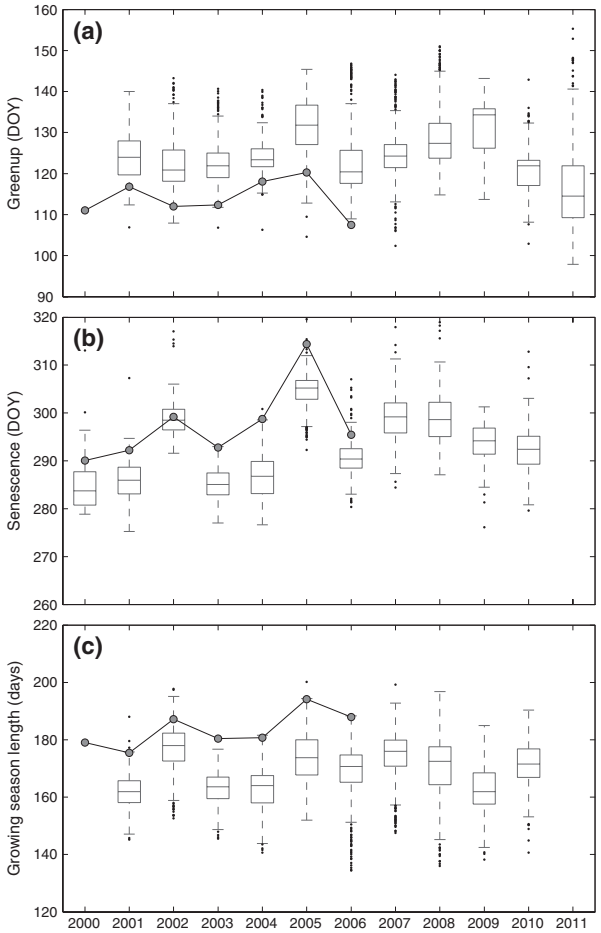

Fig. 4 Boxplots of mid-days of (a) greenup (Mid_{on}; day of year, DOY) and (b) senescence (Mid_{off}; DOY) periods, and (c) growing season length (days) from the MODIS NDVI within the study site (n = 335) since 2000. Filled dots represent the phenological signals from the 8-km GIMMS NDVI (1982–2006). Boxes have lines at the medians (50th), lower (25th), and upper (75th) quartiles, with the whiskers extended to 1.5 times the interquartile ranges. Outliers are displayed with black dots.

for two reasons. First, MODIS-derived phenology shows an averaged signal over the satellite field-of-view, mostly driven by drought-deciduous tree species in the study site (*Acer rubrum*, *Nyssa sylvatica*, and *Liriodendron tulipifera* etc.) (Ford *et al.*, 2011a; Hoffmann *et al.*, 2011). Therefore, the effect of drought stress would be mitigated at the landscape level compared to the species level. Second, the asymptotic response of the offset of leaf senescence at low elevation to plant water stress might be because the senescence timing at mid-elevation was also affected by the severe drought. This is closely related to the reverse pattern of senescence with elevation (Fig. 1a), when the water-related control on senescence is more dominant than temperature over the whole elevation gradient.

Late growing season drought in humid temperate forests

Despite ca. 2 m mean annual precipitation at low elevation, drainage efficiency and high cumulative evaporative demand yield moisture stress toward the end of the growing season in dry years. Although there is no Hortonian overland flow in these steep forested catchments, there is a sizeable amount of lateral drainage through macro-pores, much of it as storm flow (Hewlett & Hibbert, 1967). Furthermore, shallow subsurface flow from unsaturated soils is a main source of sustained base flow (Hewlett & Hibbert, 1963), tightly coupled with available water for shallow-rooted trees (<1.0 m) in the study site (Hales *et al.*, 2009). There have been studies showing that there were significant ecophysiological adjustments (Ford *et al.*, 2011a), population dynamics (Clark *et al.*, 2011), and increased mortality (Clinton *et al.*, 2003) to declining soil moisture in the study site. For this reason, soil moisture has been known to be an important structuring element for landscape-scale forest community and biodiversity (Whittaker, 1956; Day & Monk, 1974; Day *et al.*, 1988). Late growing season drought results in earlier senescence for drought-deciduous trees at low elevations and a nonlinear senescence timing with elevation, as low- and high-elevation forests experience different levels of water stress. Several experimental studies in southern Appalachians also reported premature senescence in dry years for drought-deciduous species from a throughfall displacement experiment (Wullschleger & Hanson, 2006), a temperature controlled experiment (Gunderson *et al.*, 2012), and a free air CO_2 enrichment experiment (Warren *et al.*, 2011). Hydroclimate controls on leaf senescence clearly demonstrate that drought stress acts as a secondary key constraint on GSL at low elevations in the study site; and both precipitation amount and pattern are important for canopy duration.

Asymmetric responses of greenup and senescence along the elevation gradient

In this study, we found the asymmetric responses between leaf greenup and senescence along the elevation gradient (Fig. 5). Specifically, we found more nonlinear and vertically fluctuating responses of senescence along the elevation than greenup. Even though cold air drainage might be one of the potential causes for these nonlinear responses along the elevation (Fisher *et al.*, 2006), this asymmetry cannot be explained by temperature alone. First, cold air drainage is typically collected along narrow drainage paths in these incised slopes rather than broadly over the landscape (Lundquist *et al.*, 2008). A previous

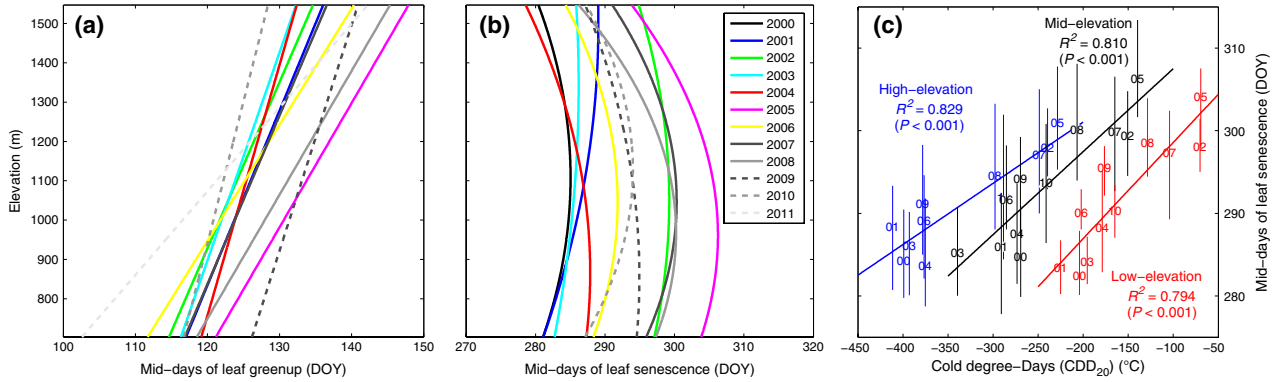

Fig. 5 Interannual variations of the MODIS-derived (a) leaf greenup and (b) senescence timing along the elevation gradient, and (c) the sensitivity of senescence to cold degree-days (CDD_{20}) during late growing season (day of year, DOY: 210–290) at three elevation regions (high: >1200 m, mid: 900–1100 m, and low: <800 m). All fitted lines are statistically significant ($P < 0.005$). Plotted numbers are the years from 2000. Vertical bars represent 5th and 95th percentiles of each group. Original plots are provided in supplementary information (Fig. S5).

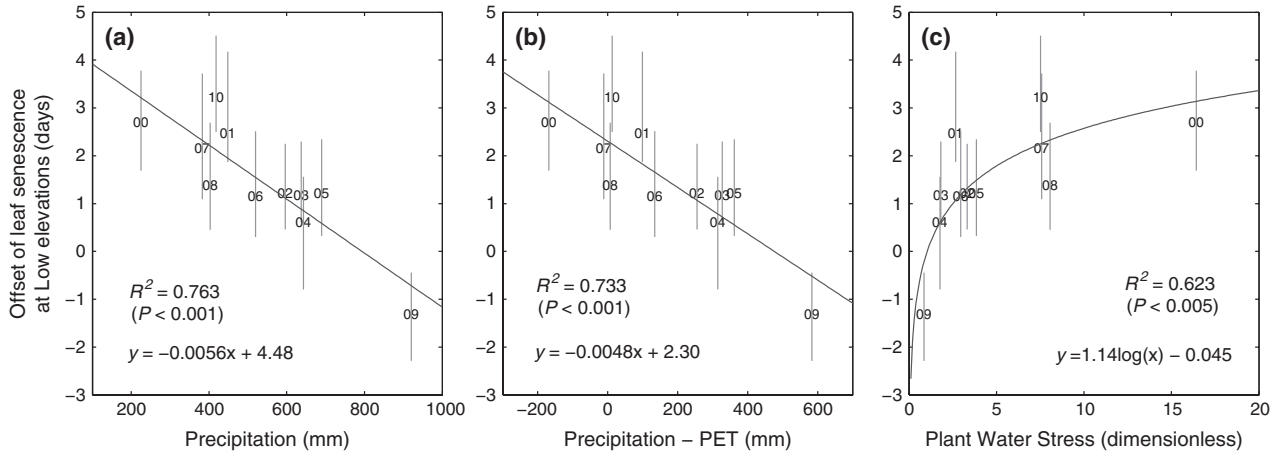

Fig. 6 Offset in the MODIS-derived leaf senescence at low elevations (<800 m; n = 41) compared with mid-elevations (900–1100 m; n = 141) vs. late growing season (July–October; a) precipitation, (b) seasonal water balance (precipitation - pan evaporation, PET) at the base station (RG06; 685 m), and (c) 60-day sum of plant water stress before senescence [Eqn (3)] from three locations in a low-elevation region (118, 218, and station 1; Fig. 1). Plotted numbers are years from 2000. Vertical bars indicate the confidence intervals for the mean differences between two groups with a paired t-test.

study in the study site and our temperature data showed that the inversion of daily min temperature along elevation only observed at valley to ridges gradients, not at the side-slopes to ridges (Bolstad *et al.*, 1998). Second, if the variations of leaf senescence along the elevation were driven by night-time temperature inversion by cold air drainage, we should have seen comparable responses in leaf greenup along the elevation. Fisher *et al.* (2006) also reported that strong negative relationships between the onset of spring and elevation at a small valley in New England, which was attributed to cold air drainage. Greenup timing in the study site might be mostly driven by temperature variations because plant available water is usually plentiful in the beginning of growing season. Furthermore, the inversion of night-time temperature by cold air drainage was reported to be more frequent without leaves in the study site (Bolstad *et al.*, 1998). Although unexpected breakpoints are also recognized in the relationships between greenup and elevation, there are little inter-annual variations in them (right above 800 m; Fig. S5). This unexpected slight delays in leaf greenup at low elevations were attributed to cold air drainage in our previous study (Hwang *et al.*, 2011), which departure from a simple linear elevation effect was well correlated to a hillslope position metric (topographic wetness index).

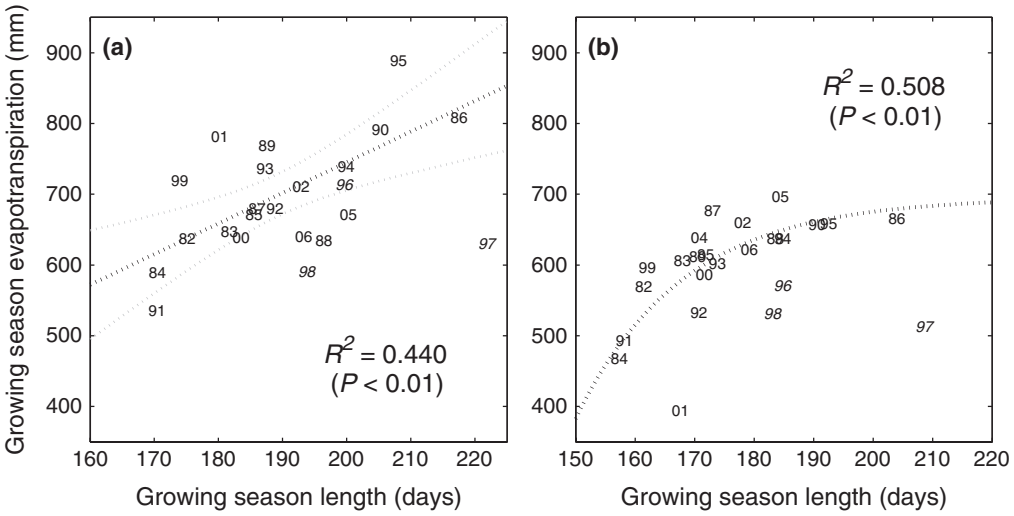

Fig. 7 The relationships between the growing season length (days) and the growing season evapotranspiration at the (a) low- (WS18 - dry) and (b) high-elevation (WS27 - wet) catchments from 1982 to 2006. Note that the points after the hurricane Opal (1996, 1997, and 1998 written in italic) were excluded in the statistical analyses because the study site experienced wide-spread canopy damages by severe wind storm.

Divergent phenological response to hydroclimate variability

This study suggests that temperature increase may have variable effects on GSL along the elevation gradient in the study site. The dominant temperature controls on senescence in temperate broadleaf trees are often adopted as simple delayed trends in senescence modeling for temperate broadleaf trees under warmer climate (Delpierre *et al*., 2009; Vitasse *et al*., 2011). Simple linear extrapolation of the effects of climate warming on leaf senescence would produce incorrect predictions in the study site. Rather, leaf senescence delay by temperature increase might be mitigated by local water availability due to increases in ET demand and drought stress toward the late growing season. The earlier senescence driven by drought stress may become more common with temperature increase and increased hydroclimate variability, possibly offsetting the influence of earlier greenup on GSL. This also presents the possibility that the forests at low elevations would move toward a state closer to a summer drought ecosystem with hydroclimate change, in which phenological controls are more dependent on interannual hydroclimate variability (Arora & Boer, 2005; Gunderson *et al*., 2012).

This mechanism provides an explanation for the lack of consistent trends in leaf senescence with climate change other than photoperiod in temperate deciduous forests. Many studies have noted that phenological responses to climate change depend not only on spring and autumn temperature, but also on winter chilling requirements (Zhang *et al*., 2007) and photoperiod (Korner & Basler, 2010). Asymmetric responses between greenup and senescence to climate change and geographic gradients have been often attributed to photoperiod controls, as photoperiod is usually assumed as a dominant autumnal trigger (White *et al*., 1997; Saxe *et al*., 2001; Schaber & Badeck, 2003). However, several papers recently reported that temperature might strongly mediate photoperiod dormancy response in deciduous woody trees (reviewed by Tanino *et al*., 2010). Dragoni & Rahman (2012) recently found that the sensitivity of the end of growing season to temperature variability was higher at low latitude regions. Gunderson *et al*. (2012) also reported a dominant temperature effect on leaf senescence from a temperature-controlled open chamber experiment in southern Appalachians. Drought stress represents the combined effect of multiple climate factors (precipitation, temperature, and radiation) with other site-specific properties (e.g., landscape position, soil texture, vegetation density etc.). This information is not usually provided with most phenological datasets, which is why we believe a few attempts to identify drought controls on leaf senescence failed especially in intersite studies (Estrella & Menzel, 2006). This study demonstrates that cumulative effects should be considered not just from thermal and radiative perspectives, but also from soil water storage especially for prospective senescence modeling.

Vegetation phenology and ecosystem water use

The GSL-ET relationships in this study demonstrate that phenological shifts driven by climate change would have different influences on ecosystem water

use and freshwater supplies between the low- and high-elevation regions. At high elevations, ecosystem water use is largely independent of GSL except during years of very short growing season, when ET was reduced. Therefore, freshwater supplies would largely depend on precipitation input patterns. However, increased precipitation would not result in the equivalent increase in runoff generation at low elevations. This study showed that freshwater availability at low elevations are more affected by ecosystem responses and feedbacks to interannual hydroclimate variability during the late growing season, which is also a critical period for freshwater supplies. This study suggests that phenological responses over topoclimate gradients would improve our understanding of a major role of vegetation in available freshwater resources to hydroclimate change in forested mountain watersheds.

We report that vegetation phenology (especially senescence) is more closely correlated with ecosystem water use at low elevations than high elevations. The critical role of phenology in stomatal conductance was observed especially for greenup in the southern Appalachians (Wilson & Baldocchi, 2000). However, drought effect on senescence and annual ET has been reported mostly in dry grasslands. At a Mediterranean grassland, Ryu *et al.* (2008) reported that annual ET was increasing by 1.6 mm with a unit increase of GSL largely determined by senescence timing. Zha *et al.* (2010) also found that drought stress controls on senescence and annual ET were stronger in grasslands and a deciduous aspen forest than in coniferous forests at the Boreal Plains. However, Richardson *et al.* (2010) could not find any significant correlation between GSL (or leaf greenup) and annual ET from the analysis of FLUXNET data for nine deciduous broadleaf forests, most of which are located at high latitudes (>40°N). These suggest that GSL might be a better indicator for ecosystem water use in water-limited ecosystems than in energy-limited ecosystems.

The GSL-ET relationships revealed the possible transient effect of major disturbances such as a major wind storm and severe drought. In years after a hurricane (1996–1998) and a historic severe drought (2001), these measures plot far below the regression lines which may indicate significant forest canopy damage. Hurricane Opal (5 October 1995) resulted in the large-scale disturbance and loss of leaf area in the study site (Clinton & Baker, 2000; Elliott *et al.*, 2002). The transient effect of severe drought is more obvious in WS27, where there is no strong storage depletion effect in ET calculation. In WS18, ET estimates [$P - Q$ in Eqn (4)] might be overestimated after a dry year as a significant portion of precipitation in the current year was still used for recharge of storage depletion from last year. On the contrary, those might be underestimated after wet dormant season due to the storage carry-over in the watershed system. Moreover, drought effect on tree mortality and growth has been more recognized around middle elevations for northern red oak (*Q. rubra*) and scarlet oak (*Q. coccinea*), where there were less frequent drought events (Clinton *et al.*, 1993; Elliott & Swank, 1994).

Landscape phenology as a diagnostic tool of forested ecosystems

The senescence trend along the elevation gradient revealed key limiting resources of vegetation; water (or covarying nitrogen) in low-elevation and energy in high-elevation regions. The variation of limiting resources along the elevation gradient in the study site has been recognized by other researchers, regarding forest community types (Day *et al.*, 1988), tree growth and fecundity (Clark *et al.*, 2011), watershed-level hydrologic behavior (Hwang *et al.*, 2012), and nitrogen mass balances (Knoepp *et al.*, 2008). It is also possible that these drought-related controls on senescence might partially result from nitrogen limitation by periodic top soil desiccation. Several studies reported that senescence was also dependent on leaf N content during late growing season (Pourtau *et al.*, 2004; Wingler *et al.*, 2006). Low-elevation forests are usually assumed to be water- or nitrogen-limited, while high-elevation northern hardwood forests are not. It is because there is strong orographic precipitation pattern along the elevation in the study site, as is N deposition (Knoepp *et al.*, 2008). Therefore, high-elevation catchments also export more nitrate in streamflow than low-elevation catchments (Block *et al.*, 2012).

Therefore, lower elevation ecosystems may be at higher risk to hydroclimate change with either increased ratios of potential evaporation to precipitation or interannual variability, such as species shifts, water scarcity, and fire hazard with change toward more xeric systems. While greenup shows a simple ecosystem response mostly to temperature variation in early growing season, senescence is sensitive to cumulative behavior in limiting resources toward the end of growing season. Covarying adiabatic temperature lapse and orographic precipitation patterns are common phenomena in mountainous terrain. In this sense, we suggest that a nonlinear response of senescence along an elevation gradient would be a simple diagnostic tool for key constraints of forest ecosystems. In this study, the elevation gradient provides a unique template to separate drought effects on leaf senescence due to concomitant temperature lapse and orographic precipitation patterns.

Note that leaf coloration itself does not represent the timing of dormancy onset or the loss of photosynthetic activity. The interannual variation of GSL is mostly determined by senescence in this study site, when photosynthetic activity is much lower than during greenup (Bauerle *et al.*, 2012). More distinct changes in canopy conductance are usually observed during greenup rather than senescence period in deciduous forests (Moore *et al.*, 1996; Wilson & Baldocchi, 2000). Richardson *et al.* (2010) also found from the FLUXNET data that gross and net ecosystem productivity are significantly correlated to the anomaly in greenup rather than to that in senescence. Although drought effect on ecosystem water use and productivity is clearly manifested in field observations (Granier *et al.*, 2007; Reichstein *et al.*, 2007; van der Molen *et al.*, 2011), remotely sensed vegetation indices often fail to capture the significant loss of photosynthetic activity especially in forested ecosystems (Hwang *et al.*, 2008).

Furthermore, landscape-scale phenological patterns upon imposed topoclimate variability are often complicated by covarying gradients, such as species patterns, hydrologic positions, and edaphic factors (Elmore *et al.*, 2012). For this reason, landscape phenology may have a limited applicability to species-level phenology models or in predicting future phenological responses to climate change. However, landscape-level phenology has been suggested to more coherently respond to topoclimate variation than plot-scale phenology (Liang & Schwartz, 2009), and provides a better understanding of key environmental controls on GSL and potential phenological responses to hydroclimate change (Hwang *et al.*, 2011; Elmore *et al.*, 2012). The landscape-induced phenological patterns are easily estimated over local mountain ranges from medium-resolution satellite products (e.g. MODIS), which may be used as a simple diagnostic for sources of ecosystem vulnerability and sensitivity to climate change.

Conclusions

For the three posed objectives in the study:

(1) The time-series of MODIS NDVI data were used to derive landscape-scale greenup and senescence patterns, which were validated with continuous FPAR and weekly phenological observations. Asymmetric patterns between greenup and senescence with elevation were shown.
(2) We demonstrate that a nonlinear response of leaf senescence along the elevation gradient was closely related to late growing season hydroclimate variability, leading to tighter coupling between vegetation duration and ecosystem water use at low elevations compared to high elevations.
(3) This study indicated a critical role of drought stress on leaf senescence in a humid temperate broadleaf forest, and potentially divergent ecosystem responses between high and low elevation forests to hydroclimate change.

The study site is located in a heavily forested region with high precipitation but also moderate temperatures, such that variation in GSL can exhaust available soil water. It is important to investigate how widespread this phenomenon is, and the implications of climate change for expanding this behavior with increasing GSL and hydroclimate variability.

Acknowledgements

The research represented in this paper was supported by a National Science Foundation award DEB-0823293 from the Long Term Ecological Research Program to the Coweeta LTER Program at the University of Georgia, and by the USDA Forest Service, Southern Research Station, Coweeta Hydrologic Laboratory. Any opinions, findings, conclusions, or recommendations expressed in the material are those of the authors and do not necessarily reflect the views of the National Science Foundation or USDA Forest Service. We thank USDA Forest Service for long-term climate and streamflow data, as well as access and facilities at the Coweeta Hydrologic Lab. We also thank the editor, Josep Peñuelas, Drs. A. Richardson, and D.S. Mackay for helpful comments on the manuscript.

References

Adams HD, Guardiola-Claramonte M, Barron-Gafford GA *et al.* (2009) Temperature sensitivity of drought-induced tree mortality portends increased regional die-off under global-change-type drought. *Proceedings of the National Academy of Sciences of the United States of America*, **106**, 7063–7066.

Angert A, Biraud S, Bonfils C *et al.* (2005) Drier summers cancel out the CO_2 uptake enhancement induced by warmer springs. *Proceedings of the National Academy of Sciences of the United States of America*, **102**, 10823–10827.

Arora VK, Boer GJ (2005) A parameterization of leaf phenology for the terrestrial ecosystem component of climate models. *Global Change Biology*, **11**, 39–59.

Barr AG, Black TA, Hogg EH, Kljun N, Morgenstern K, Nesic Z (2004) Interannual variability in the leaf area index of a boreal aspen-hazelnut forest in relation to net ecosystem production. *Agricultural and Forest Meteorology*, **126**, 237–255.

Bauerle WL, Oren R, Way DA *et al.* (2012) Photoperiodic regulation of the seasonal pattern of photosynthetic capacity and the implications for carbon cycling. *Proceedings of the National Academy of Sciences of the United States of America*, **109**, 8612–8617.

Black TA, Chen WJ, Barr AG *et al.* (2000) Increased carbon sequestration by a boreal deciduous forest in years with a warm spring. *Geophysical Research Letters*, **27**, 1271–1274.

Block CE, Knoepp JD, Elliott KJ, Fraterrigo JM (2012) Impacts of hemlock loss on nitrogen retention vary with soil nitrogen availability in the southern Appalachian mountains. *Ecosystems*, **15**, 1108–1120.

Bolstad PV, Swift L, Collins F, Regniere J (1998) Measured and predicted air temperatures at basin to regional scales in the southern Appalachian mountains. *Agricultural and Forest Meteorology*, **91**, 161–176.

Chen WJ, Black TA, Yang PC *et al.* (1999) Effects of climatic variability on the annual carbon sequestration by a boreal aspen forest. *Global Change Biology*, **5**, 41–53.

Chuine I, Beaubien EG (2001) Phenology is a major determinant of tree species range. *Ecology Letters*, **4**, 500–510.

Churkina G, Schimel D, Braswell BH, Xiao XM (2005) Spatial analysis of growing season length control over net ecosystem exchange. *Global Change Biology*, **11**, 1777–1787.

Clark JS, Bell DM, Hersh MH, Nichols L (2011) Climate change vulnerability of forest biodiversity: climate and competition tracking of demographic rates. *Global Change Biology*, **17**, 1834–1849.

Clinton B, Baker C (2000) Catastrophic windthrow in the southern Appalachians: characteristics of pits and mounds and initial vegetation responses. *Forest Ecology and Management*, **126**, 51–60.

Clinton BD, Boring LR, Swank WT (1993) Canopy gap characteristics and drought influences in oak forests of the Coweeta Basin. *Ecology*, **74**, 1551–1558.

Clinton BD, Yeakley JA, Apsley DK (2003) Tree growth and mortality in a southern Appalachian deciduous forest following extended wet and dry periods. *Castanea*, **68**, 189–200.

Day FP, Monk CD (1974) Vegetation patterns on a southern Appalachian watershed. *Ecology*, **55**, 1064–1074.

Day FP, Philips DL, Monk CD (1988) Forest communities and patterns. In: *Forest Hydrology and Ecology at Coweeta* (eds Swank WT, Crossley JDA), pp. 141–149. Springer-Verlag, New York, NY.

Delpierre N, Dufrene E, Soudani K, Ulrich E, Cecchini S, Boe J, Francois C (2009) Modelling interannual and spatial variability of leaf senescence for three deciduous tree species in France. *Agricultural and Forest Meteorology*, **149**, 938–948.

Doi H, Takahashi M (2008) Latitudinal patterns in the phenological responses of leaf colouring and leaf fall to climate change in Japan. *Global Ecology and Biogeography*, **17**, 556–561.

Dragoni D, Rahman AF (2012) Trends in fall phenology across the deciduous forests of the Eastern USA. *Agricultural and Forest Meteorology*, **157**, 96–105.

Elliott KJ, Swank WT (1994) Impacts of drought on tree mortality and growth in a mixed hardwood forest. *Journal of Vegetation Science*, **5**, 229–236.

Elliott KJ, Hitchcock SL, Krueger L (2002) Vegetation response to large scale disturbance in a southern Appalachian forest: hurricane Opal and salvage logging. *Journal of the Torrey Botanical Society*, **129**, 48–59.

Elmore AJ, Guinn SM, Minsley BJ, Richardson AD (2012) Landscape controls on the timing of spring, autumn, and growing season length in mid-Atlantic forests. *Global Change Biology*, **18**, 656–674.

Estrella N, Menzel A (2006) Responses of leaf colouring in four deciduous tree species to climate and weather in Germany. *Climate Research*, **32**, 253–267.

Fisher JI, Mustard JF, Vadeboncoeur MA (2006) Green leaf phenology at Landsat resolution: scaling from the field to the satellite. *Remote Sensing of Environment*, **100**, 265–279.

Ford CR, Hubbard RM, Kloeppel BD, Vose JM (2007) A comparison of sap flux-based evapotranspiration estimates with catchment-scale water balance. *Agricultural and Forest Meteorology*, **145**, 176–185.

Ford CR, Hubbard RM, Vose JM (2011a) Quantifying structural and physiological controls on variation in canopy transpiration among planted pine and hardwood species in the southern Appalachians. *Ecohydrology*, **4**, 183–195.

Ford CR, Laseter SH, Swank WT, Vose JM (2011b) Can forest management be used to sustain water-based ecosystem services in the face of climate change? *Ecological Applications*, **21**, 2049–2067.

Goulden ML, Munger JW, Fan SM, Daube BC, Wofsy SC (1996) Exchange of carbon dioxide by a deciduous forest: response to interannual climate variability. *Science*, **271**, 1576–1578.

Granier A, Reichstein M, Breda N *et al.* (2007) Evidence for soil water control on carbon and water dynamics in European forests during the extremely dry year: 2003. *Agricultural and Forest Meteorology*, **143**, 123–145.

Gunderson CA, Edwards NT, Walker AV, O'Hara KH, Campion CM, Hanson PJ (2012) Forest phenology and a warmer climate - growing season extension in relation to climatic provenance. *Global Change Biology*, **18**, 2008–2025.

Gupta RK, Vijayan D, Prasad TS, Tirumaladevi NC (2000) Role of bandwidth in computation of NDVI from Landsat TM and NOAA AVHRR bands. *Remote Sensing for Land Surface Characterisation*, **26**, 1141–1144.

Hales TC, Ford CR, Hwang T, Vose JM, Band LE (2009) Topographic and ecologic controls on root reinforcement. *Journal of Geophysical Research-Earth Surface*, **114**, F03013.

Hanninen H, Tanino K (2011) Tree seasonality in a warming climate. *Trends in plant science*, **16**, 412–416.

Hewlett JD, Hibbert AR (1963) Moisture and energy conditions within a sloping soil mass during drainage. *Journal of Geophysical Research*, **68**, 1081–1087.

Hewlett JD, Hibbert AR (1967) Factors affecting the response of small watersheds to precipitation in humid areas. In: *Forest Hydrology* (eds Sopper NE, Lull HW), pp. 275–290. Pergamon Press, New York.

Hoffmann WA, Marchin RM, Abit P, Lau OL (2011) Hydraulic failure and tree dieback are associated with high wood density in a temperate forest under extreme drought. *Global Change Biology*, **17**, 2731–2742.

Hopkins AD (1918) Periodical events and natural law as guides to agricultural research and practice. *Monthly Weather Review*, **9**(Suppl.), 1–42.

Hu J, Moore D, Burns SP, Monson RK (2010) Longer growing seasons lead to less carbon sequestration by a subalpine forest. *Global Change Biology*, **16**, 771–783.

Hwang T, Kang S, Kim J, Kim Y, Lee D, Band L (2008) Evaluating drought effect on MODIS Gross Primary Production (GPP) with an eco-hydrological model in the mountainous forest, East Asia. *Global Change Biology*, **14**, 1037–1056.

Hwang T, Band LE, Hales TC (2009) Ecosystem processes at the watershed scale: extending optimality theory from plot to catchment. *Water Resources Research*, **45**, W11425.

Hwang T, Song C, Vose JM, Band LE (2011) Topography-mediated controls on local vegetation phenology estimated from MODIS vegetation index. *Landscape Ecology*, **26**, 541–556.

Hwang T, Band LE, Vose JM, Tague C (2012) Ecosystem processes at the watershed scale: hydrologic vegetation gradient as an indicator for lateral hydrologic connectivity of headwater catchments. *Water Resources Research*, **48**, W06514.

Jeong S, Ho C, Gim H, Brown ME (2011) Phenology shifts at start vs. end of growing season in temperate vegetation over the Northern Hemisphere for the period 1982-2008. *Global Change Biology*, **17**, 2385–2399.

Jolly WM, Nemani R, Running SW (2005) A generalized, bioclimatic index to predict foliar phenology in response to climate. *Global Change Biology*, **11**, 619–632.

Jung M, Reichstein M, Ciais P *et al.* (2010) Recent decline in the global land evapotranspiration trend due to limited moisture supply. *Nature*, **467**, 951–954.

Knoepp JD, Vose JM, Swank WT (2008) Nitrogen deposition and cycling across an elevation and vegetation gradient in southern Appalachian forests. *International Journal of Environmental Studies*, **65**, 389–408.

Korner C, Basler D (2010) Phenology under global warming. *Science*, **327**, 1461–1462.

Kramer K (1995) Phenotypic plasticity of the phenology of 7 European tree species in relation to climatic warming. *Plant Cell and Environment*, **18**, 93–104.

Laio F, Porporato A, Ridolfi L, Rodriguez-Iturbe I (2001) Plants in water-controlled ecosystems: active role in hydrologic processes and response to water stress - II. Probabilistic soil moisture dynamics. *Advances in Water Resources*, **24**, 707–723.

Lers A (2007) Environmental regulation of leaf senescence. In: *Annual Plant Reviews (Series)* (ed Gan S), pp. 108–144. Blackwell Publishing Ltd., New York.

Liang L, Schwartz MD (2009) Landscape phenology: an integrative approach to seasonal vegetation dynamics. *Landscape Ecology*, **24**, 465–472.

Liang L, Schwartz MD, Fei S (2011) Validating satellite phenology through intensive ground observation and landscape scaling in a mixed seasonal forest. *Remote Sensing of Environment*, **115**, 143–157.

Lundquist JD, Pepin N, Rochford C (2008) Automated algorithm for mapping regions of cold-air pooling in complex terrain. *Journal of Geophysical Research: Atmospheres (1984–2012)*, **113**, D22.

Marchin R, Zeng H, Hoffmann W (2010) Drought-deciduous behavior reduces nutrient losses from temperate deciduous trees under severe drought. *Oecologia*, **163**, 845–854.

Menzel A, Sparks TH, Estrella N *et al.* (2006) European phenological response to climate change matches the warming pattern. *Global Change Biology*, **12**, 1969–1976.

van der Molen MK, Dolman AJ, Ciais P *et al.* (2011) Drought and ecosystem carbon cycling. *Agricultural and Forest Meteorology*, **151**, 765–773.

Moore KE, Fitzjarrald DR, Sakai RK, Goulden ML, Munger JW, Wofsy SC (1996) Seasonal variation in radiative and turbulent exchange at a deciduous forest in central Massachusetts. *Journal of Applied Meteorology*, **35**, 122–134.

Munne-Bosch S, Alegre L (2004) Die and let live: leaf senescence contributes to plant survival under drought stress. *Functional Plant Biology*, **31**, 203–216.

O'Gorman PA, Schneider T (2009) The physical basis for increases in precipitation extremes in simulations of 21st-century climate change. *Proceedings of the National Academy of Sciences of the United States of America*, **106**, 14773–14777.

Partanen J, Koski V, Hanninen H (1998) Effects of photoperiod and temperature on the timing of bud burst in Norway spruce (Picea abies). *Tree physiology*, **18**, 811–816.

Pataki DE, Oren R (2003) Species differences in stomatal control of water loss at the canopy scale in a mature bottomland deciduous forest. *Advances in Water Resources*, **26**, 1267–1278.

Porporato A, Laio F, Ridolfi L, Rodriguez-Iturbe I (2001) Plants in water-controlled ecosystems: active role in hydrologic processes and response to water stress - III. Vegetation water stress. *Advances in Water Resources*, **24**, 725–744.

Pourtau N, Mares M, Purdy S, Quentin N, Ruel A, Wingler A (2004) Interactions of abscisic acid and sugar signalling in the regulation of leaf senescence. *Planta*, **219**, 765–772.

Prebyl TJ (2012) An analysis of the patterns and processes associated with spring forest phenology in a southern Appalachian landscape using remote sensing. Master's thesis, University of Georgia. Athens, GA.

Reichstein M, Ciais P, Papale D *et al*. (2007) Reduction of ecosystem productivity and respiration during the European summer 2003 climate anomaly: a joint flux tower, remote sensing and modelling analysis. *Global Change Biology*, **13**, 634–651.

Richardson AD, Bailey AS, Denny EG, Martin CW, O'Keefe J (2006) Phenology of a northern hardwood forest canopy. *Global Change Biology*, **12**, 1174–1188.

Richardson AD, Black TA, Ciais P *et al*. (2010) Influence of spring and autumn phenological transitions on forest ecosystem productivity. *Philosophical Transactions of the Royal Society B-Biological Sciences*, **365**, 3227–3246.

Rivero RM, Kojima M, Gepstein A, Sakakibara H, Mittler R, Gepstein S, Blumwald E (2007) Delayed leaf senescence induces extreme drought tolerance in a flowering plant. *Proceedings of the National Academy of Sciences of the United States of America*, **104**, 19631–19636.

Rodriguez-Iturbe I, D'Odorico P, Porporato A, Ridolfi L (1999) On the spatial and temporal links between vegetation, climate, and soil moisture. *Water Resources Research*, **35**, 3709–3722.

Ryu Y, Baldocchi DD, Ma S, Hehn T (2008) Interannual variability of evapotranspiration and energy exchange over an annual grassland in California. *Journal of Geophysical Research-Atmospheres*, **113**, D09104.

Saxe H, Cannell MG, Johnsen Ø, Ryan MG, Vourlitis G (2001) Tree and forest functioning in response to global warming. *New Phytologist*, **149**, 369–399.

Schaber J, Badeck FW (2003) Physiology-based phenology models for forest tree species in Germany. *International Journal of Biometeorology*, **47**, 193–201.

Schimel D, Kittel TGF, Running S, Monson R, Turnispeed A, Anderson D (2002) Carbon sequestration studied in western U.S. mountains. *EOS Transactions*, **83**, 445.

Schwartz MD, Hanes JM (2010) Continental-scale phenology: warming and chilling. *International Journal of Climatology*, **30**, 1595–1598.

Seager R, Tzanova A, Nakamura J (2009) Drought in the Southeastern United States: causes, variability over the last millennium, and the potential for future hydroclimate change. *Journal of Climate*, **22**, 5021–5045.

Swift LW, Cunningham GB, Douglass JE (1988) Climatology and hydrology. In: *Forest Hydrology and Ecology at Coweeta* (eds Swank WT, Crossley JDA), pp. 35–55. Springer-Verlag, New York.

Tanino KK, Kalcsits L, Silim S, Kendall E, Gray GR (2010) Temperature-driven plasticity in growth cessation and dormancy development in deciduous woody plants: a working hypothesis suggesting how molecular and cellular function is affected by temperature during dormancy induction. *Plant Molecular Biology*, **73**, 49–65.

Teillet PM, Fedosejevs G, Thome KJ, Barker JL (2007) Impacts of spectral band difference effects on radiometric cross-calibration between satellite sensors in the solar-reflective spectral domain. *Remote Sensing of Environment*, **110**, 393–409.

Troch PA, Martinez GF, Pauwels VRN *et al*. (2009) Climate and vegetation water use efficiency at catchment scales. *Hydrological Processes*, **23**, 2409–2414.

Tucker CJ, Pinzon JE, Brown ME *et al*. (2005) An extended AVHRR 8-km NDVI dataset compatible with MODIS and SPOT vegetation NDVI data. *International Journal of Remote Sensing*, **26**, 4485–4498.

Vitasse Y, Bresson CC, Kremer A, Michalet R, Delzon S (2010) Quantifying phenological plasticity to temperature in two temperate tree species. *Functional Ecology*, **24**, 1211–1218.

Vitasse Y, Francois C, Delpierre N, Dufrene E, Kremer A, Chuine I, Delzon S (2011) Assessing the effects of climate change on the phenology of European temperate trees. *Agricultural and Forest Meteorology*, **151**, 969–980.

Viviroli D, Durr HH, Messerli B, Meybeck M, Weingartner R (2007) Mountains of the world, water towers for humanity: typology, mapping, and global significance. *Water Resources Research*, **43**, W07447.

Warren JM, Norby RJ, Wullschleger SD (2011) Elevated CO_2 enhances leaf senescence during extreme drought in a temperate forest. *Tree Physiology*, **31**, 117–130.

White MA, Nemani AR (2003) Canopy duration has little influence on annual carbon storage in the deciduous broad leaf forest. *Global Change Biology*, **9**, 967–972.

White MA, Thornton PE, Running SW (1997) A continental phenology model for monitoring vegetation responses to interannual climatic variability. *Global Biogeochemical Cycles*, **11**, 217–234.

White MA, de Beurs KM, Didan K *et al*. (2009) Intercomparison, interpretation, and assessment of spring phenology in North America estimated from remote sensing for 1982-2006. *Global Change Biology*, **15**, 2335–2359.

Whittaker RH (1956) Vegetation of the Great Smoky Mountains. *Ecological Monographs*, **26**, 1–69.

Wilson KB, Baldocchi DD (2000) Seasonal and interannual variability of energy fluxes over a broadleaved temperate deciduous forest in North America. *Agricultural and Forest Meteorology*, **100**, 565–578.

Wingler A, Purdy S, MacLean JA, Pourtau N (2006) The role of sugars in integrating environmental signals during the regulation of leaf senescence. *Journal of experimental botany*, **57**, 391–399.

Wullschleger SD, Hanson PJ (2006) Sensitivity of canopy transpiration to altered precipitation in an upland oak forest: evidence from a long-term field manipulation study. *Global Change Biology*, **12**, 97–109.

Yang X, Mustard JF, Tang J, Xu H (2012) Regional-scale phenology modeling based on meteorological records and remote sensing observations. *Journal of Geophysical Research-Biogeosciences*, **117**, G03029.

Zha T, Barr AG, van der Kamp G, Black TA, McCaughey JH, Flanagan LB (2010) Interannual variation of evapotranspiration from forest and grassland ecosystems in Western Canada in relation to drought. *Agricultural and Forest Meteorology*, **150**, 1476–1484.

Zhang X, Goldberg MD (2011) Monitoring fall foliage coloration dynamics using time-series satellite data. *Remote Sensing of Environment*, **115**, 382–391.

Zhang XY, Friedl MA, Schaaf CB (2006) Global vegetation phenology from Moderate Resolution Imaging Spectroradiometer (MODIS): evaluation of global patterns and comparison with in situ measurements. *Journal of Geophysical Research-Biogeosciences*, **111**, G04017.

Zhang X, Tarpley D, Sullivan JT (2007) Diverse responses of vegetation phenology to a warming climate. *Geophysical Research Letters*, **34**, L19405.

Zhao MS, Running SW (2010) Drought-induced reduction in global terrestrial net primary production from 2000 through 2009. *Science*, **329**, 940–943.

Supporting Information

Additional Supporting Information may be found in the online version of this article:

Figure S1. (a) Annual and late growing-season (July–October; green) precipitation and pan evaporation (reverse *y*-axis) patterns at the base climate station (RG06; 685 m). (b) Monthly mean precipitation and pan evaporation (reverse *y*-axis) during the last decade (2000–2010). Colored bars are from RG06, while blank ones from the highest rain gauge (RG31; 1363 m) within the study site. Vertical bars represent the standard deviations. (c) The scatter plot of monthly precipitation between two rain gauges (RG06, RG31) from 2000. All units are mm. Reprinted from Hwang *et al.* (2012).
Figure S2. The time series of MODIS Normalized Difference Vegetation Index (NDVI) values (open symbols) and fitted logistic functions (lines) at five selected MODIS pixels within the study site. Reprinted from Hwang *et al.* (2011).
Figure S3. (a) Temporal patterns of phenological indices (0–1, symbols) and fitted logistic functions (lines, greenup - green, coloration - red, and abscission - blue), (b) interannual variations of leaf greenup, (c) coloration, and (d) abscission at the low-elevation walk-up tower (station 2; Table 2; Fig. 1).
Figure S4. (a) Temporal patterns of Fraction of absorbed Photosynthetically Active Radiation (FPAR, symbols) and nonlinear logistic fits (lines), (b) interannual variations of leaf greenup, and (c) senescence at the low-elevation walk-up tower (station 2; Table 2; Fig. 1).
Figure S5. Interannual variations of mid-days of greenup (Mid_{on}; DOY) and senescence (Mid_{off}; DOY) phenology along the elevation gradient from 2000, estimated from time-series of MODIS NDVI. Each point represents each MODIS pixel. All fitted lines are statistically significant ($P < 0.005$). Black filled points represent observed vegetation phenology from FPAR at two walk-up towers (Table 2; Fig. 1).
Figure S6. Time series and cumulative distribution plots of observed soil water content at (a) 118, (b) 218, (c) 318, (d) 427, (e) 527, (f) station 1, (g) station 2, (h) station 3, and (i) station 4. Only 118, 218, and station 1 data at the low-elevation region (<800 m) were used to calculate the plant water stress values in Fig. 6c. Geographical locations and detailed explanations of these sites are available in Fig. 1 and Table 2.
Figure S7. (a) The time-series of bi-monthly 8-km Global Inventory Modeling and Mapping Studies (GIMMS) NDVI from 1982 to 2006 around the study site. Filled black dots represent the data points excluded by the two-step filtering technique (Hwang *et al.*, 2011). Mid-days of (b) leaf greenup and (c) senescence (as Day of Year, DOY) from estimated from the intersections between the midpoint NDVI (a horizontal line) and time-series of NDVI lines. Open circles represent the phenological signals from the adjacent eight GIMMS NDVI pixels in the 3-by-3 window.